AeroRib-FDLC-X

A Graded Riblet / Low-Fluorine Diamond-Like Carbon Hybrid Surface for Aircraft Drag Reduction

Physics-corrected redesign and falsification study of the 2025 AeroDLC-F proposal

Technical concept paper | September 4, 2026

Status: engineering hypothesis, not a validated or certified aircraft material

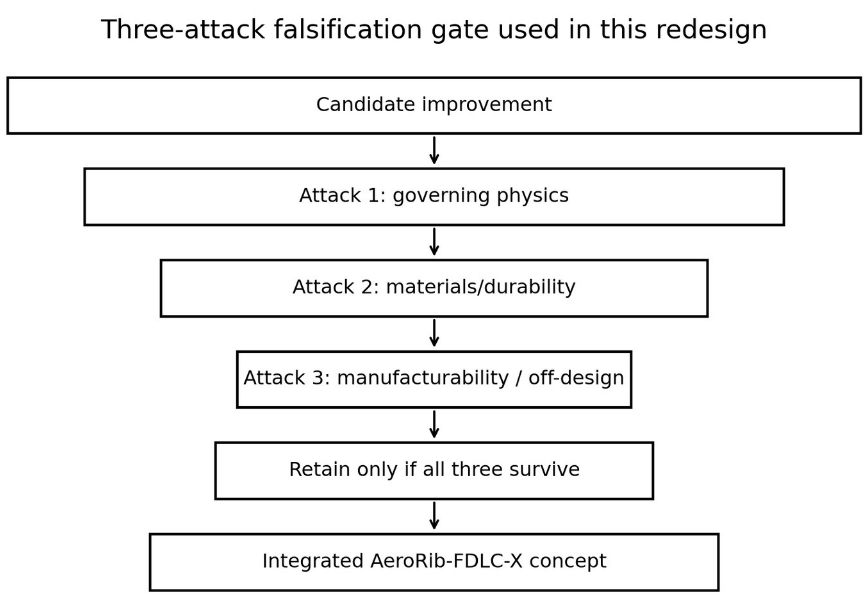

Figure 1. The redesign uses a three-attack falsification gate for every proposed improvement.

Important qualification. A desk analysis can reject internally inconsistent ideas, but it cannot prove flight performance. In this paper, “passes” means that an idea survives three independent analytical attacks well enough to justify coupon, wind-tunnel, erosion, and ultimately flight testing. No numerical drag or fuel claim in this document should be treated as certified performance before those tests are completed.

Abstract

The source AeroDLC-F paper proposes a fluorinated diamond-like carbon (F-DLC) coating with a low solid-on-solid coefficient of friction and then infers a reduction in aircraft skin-friction drag. The inference is not physically sufficient: aerodynamic skin friction is wall shear in a viscous boundary layer and is quantified by the fluid-mechanical skin-friction coefficient Cf, not by the dry sliding tribological coefficient measured against steel. This redesign therefore changes the primary mechanism rather than merely tuning the original chemistry. The proposed AeroRib-FDLC-X architecture uses flow-aligned micro-riblets, locally scaled in viscous wall units and oriented to computed surface streamlines, as the direct drag-reduction mechanism. A thin, low-fluorine, multilayer DLC nanocoating is retained as a secondary functional layer to protect riblet geometry, lower surface energy, reduce contamination adhesion, and improve wear resistance. The architecture is implemented as a removable, microreplicated film so the airframe does not require whole-wing vacuum processing.

Seven candidate improvements were examined. Increased fluorination, graphene/fluorographene as a primary aerodynamic layer, and superhydrophobic micro/nanotexturing as a direct drag device were rejected after three independent attacks each. Four improvements survived at the concept level: conventional straight riblets, zonally graded riblet scale/orientation, a low-fluorine multilayer DLC protective cap, and a replaceable film architecture. A first-order aircraft model predicts that if skin friction is 40-50% of cruise drag, 65-80% of the skin-friction-producing area is effectively treated, and riblets deliver 6-8% local skin-friction reduction with realistic installation losses, aircraft-level cruise drag reduction of roughly 1.3-2.5% is plausible. This range is intentionally consistent with published riblet literature and current commercial sharkskin-film experience rather than the unsubstantiated 5% total-drag claim in the source paper. The paper gives governing equations, chemistry targets, process windows, geometrical design rules, manufacturing instructions, failure criteria, a validation matrix, and a staged certification roadmap.

1. Scope, source paper, and redesign objective

The source document is “AeroDLC-F: A Novel Perfluorinated Diamond-Like Carbon Coating for Aerodynamic Friction Reduction on Airplane Wings,” dated 27 August 2025 and distributed through EquationFarm. It specifies an amorphous carbon film with nominally 10-20 at.% fluorine, 1-5 micrometers thickness, hardness of 15-25 GPa, and a dry sliding coefficient of friction around 0.03. It proposes PECVD using CF_4 and C_2H_2, a metallic or SiC interlayer, and claims 1-5% fuel improvement with a 5% drag-reduction peak near Mach 0.8 [1].

The redesign objective is not to maximize an isolated “slipperiness” metric. It is to maximize verified aircraft energy benefit after accounting for boundary-layer physics, surface roughness, contamination, rain/sand erosion, thermal cycling, installation tolerances, added mass, maintenance, environmental burden, and certification. The resulting concept is intentionally more conservative in headline drag reduction but dramatically stronger in causal validity and testability.

2. Critical audit of the original AeroDLC-F hypothesis

Issue	Why it matters	Consequence for redesign
Tribological CoF is treated as aerodynamic skin friction	A dry sliding CoF against steel describes a contacting solid tribopair. Aerodynamic Cf is wall shear normalized by dynamic pressure. The quantities are not interchangeable [2,3].	Do not use low solid-solid CoF as the primary drag mechanism.

No boundary-layer scaling	Drag reduction is claimed as a function of Mach without showing Reynolds number, wall shear, pressure gradient, roughness, or transition state.	Use wall-unit scaling s+, h+, Reynolds number, and local surface streamlines.
Unsubstantiated “5% drag” curve	The source says CFD was used but provides no mesh, turbulence model, geometry, uncertainty, or numerical data, and the displayed PDF contains no actual plotted curve.	Replace with transparent first-order equations and define required CFD/wind-tunnel validation.
Very high sp3 fraction stated with modest hardness	F-DLC literature shows fluorine generally shifts the carbon network and can reduce hardness as F rises [10,11].	Use a graded stack: tough DLC underlayer, low-F cap only where surface chemistry is needed.
Whole-aircraft PECVD scalability is asserted, not demonstrated	A vacuum PECVD chamber for completed wings/fuselage is impractical compared with an installable film. “Robotic spraying” is not the same process as PECVD.	Manufacture coated riblet film off-aircraft in roll form; install during maintenance.
CF4 process burden omitted	CF4 is an extremely long-lived greenhouse gas with very high GWP [18].	Minimize fluorine dose, use abatement/closed-loop process development, and treat CF4 as an R&D baseline rather than preferred production chemistry.
Durability and contamination omitted	Riblet-size surface features are vulnerable to dirt, erosion, paint steps, seams, and misalignment.	Make durability, roughness, cleaning, and repair part of the core design.

2.1 Governing distinction: tribological friction versus aerodynamic skin friction

The essential correction is mathematical. For external aerodynamics, wall shear stress tau_w and the skin-friction coefficient Cf are related by [3]:

$$Cf = tau\_w / q = 2\ tau\_w / (rho\ U^2), \qquad \text{where } q = (1/2)\ rho\ U^2.$$

For a smooth turbulent flat-plate approximation, an often-used compressible engineering correlation is:

$$Cf\_bar \approx 0.455 / [(\log10\ Re\_L)^{2.58} (1 + 0.144\ M^2)^{0.65}].$$

The original 0.03 dry sliding CoF is therefore neither the value of aerodynamic Cf nor a multiplicative scaling for Cf. A low-energy smooth coating can still matter indirectly by controlling roughness, contamination, water/ice adhesion, and durability, but it does not create a direct 10x aerodynamic benefit merely because 0.03 is smaller than a PTFE sliding coefficient.

3. Redesign strategy: separate the direct and indirect mechanisms

AeroRib-FDLC-X separates functions that the original paper conflated. The direct aerodynamic mechanism is riblet geometry. The indirect material mechanism is a durable, low-energy protective surface. This separation allows every performance claim to be traced to a governing physical variable.

Function	Primary design variable	Mechanism	Verification metric
Direct skin-friction reduction	Riblet spacing s, height h, tip/root geometry, orientation	Restricts near-wall cross-stream motion and alters turbulent momentum transfer [4-7].	Delta Cf/Cf in wind tunnel or flight.

Off-design robustness	Zone-specific s+ and local streamline orientation	Keeps riblets near their effective wall-unit range and avoids yaw loss.	s+ envelope and misalignment distribution.
Geometry retention	DLC/DLN/F-DLC stack thickness, modulus, adhesion, stress	Hard nanolayers resist rounding, abrasion and chemical attack.	Profilometry after erosion/cleaning cycles.
Anti-fouling / low surface energy	Top-layer F content and surface bonding	Reduces adhesion of water and contaminants; may aid insect/ice residue release [10,15-17].	Surface energy, contact-angle hysteresis, residue removal force.
Maintainability	Removable film, seam design, panel zoning	Allows replacement without vacuum-processing the aircraft.	Install time, peel strength, repair time, seam roughness.

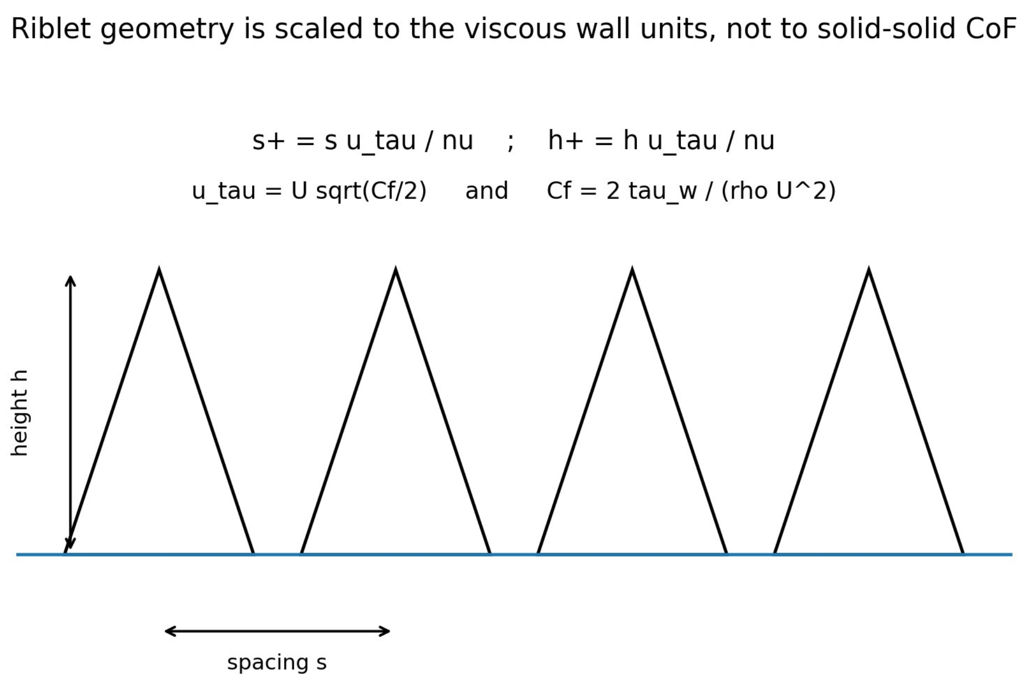

Figure 2. The principal aerodynamic geometry is set in viscous wall units. The wall shear state determines physical riblet size.

4. Candidate improvement falsification program

Each improvement idea below was subjected to exactly three attacks. An idea is rejected if any attack exposes a mechanism-level contradiction that cannot be repaired without changing the idea. Accepted ideas still require experiment.

4.1 Idea A - Increase fluorine content until F-DLC is “more slippery” than PTFE

Attack	Attempt to discredit	Result
A1 - Aerodynamic relevance	Even a spectacular reduction in ball-on-disk CoF does not establish lower gas-side wall shear; no-slip boundary-layer physics remains.	FAIL. Primary premise is not the aerodynamic mechanism.

A2 - Mechanical tradeoff	F-DLC reviews report that increasing F generally reduces sp3 cross-linking, hardness and elastic recovery; high-F films can become polymer-like [10,11].	FAIL. More F can make the surface less durable.
A3 - Process/environment	CF_4 and other PFC feed gases impose significant greenhouse-gas and abatement burdens [18].	FAIL. “More F” worsens manufacturing externalities.

Verdict: REJECT as a drag-improvement strategy. Retain only a thin, low-F cap whose purpose is surface energy and contamination control.

4.2 Idea B - Add graphene or fluorographene as the primary “super-slippery” aerodynamic layer

Attack	**Attempt to discredit**	**Result**
B1 - Governing physics	Atomically low solid friction does not remove the no-slip boundary condition for ordinary external airflow.	FAIL as a direct drag mechanism.
B2 - Scale-up integrity	Large aircraft surfaces would contain grain boundaries, wrinkles, pinholes, seams, and substrate roughness; these can dominate the aerodynamic roughness budget.	FAIL at aircraft scale without a separate smoothing architecture.
B3 - Materials integration	Conductive graphitic layers on aluminum require careful galvanic isolation; brittle ultrathin coatings also face rain/particle erosion and repair challenges.	FAIL the maintenance/robustness screen.

Verdict: REJECT as the primary aerodynamic upgrade. Graphitic carbon remains naturally present in the sp2 fraction of DLC, but a discrete graphene film is not required for the proposed concept.

4.3 Idea C - Add superhydrophobic micro/nanotexture to trap air and reduce drag

Attack	**Attempt to discredit**	**Result**
C1 - Medium mismatch	Gas-side drag reduction from superhydrophobic air pockets is not analogous to liquid-flow slip; in external air, added texture is primarily roughness.	FAIL as a direct drag device.
C2 - Roughness penalty	Random or isotropic micro/nanotexture can increase turbulent skin friction and trigger transition; it competes with the carefully sized riblet geometry.	FAIL unless texture amplitude is far below the aerodynamic roughness budget.
C3 - Icing/erosion stability	Published icing work shows wetting state changes during cooling, while high-speed rain/particle impact can damage structured surfaces [16,17].	FAIL as the main mechanism.

Verdict: REJECT as a direct drag technology. Hydrophobic chemistry may be retained on an otherwise aerodynamically controlled surface.

4.4 Idea D - Use conventional straight riblets aligned to local flow

Attack	Attempt to discredit	Result
D1 - Is the mechanism real?	NASA flight tests and decades of experiments report roughly 4-8% turbulent skin-friction reductions when riblets are properly sized; reviews report up to about 10% under optimized conditions [4-7].	PASS.
D2 - Yaw sensitivity	2024 experiments found about 7% maximum drag reduction and little attenuation below ~10 degrees yaw, but rapid loss by ~15 degrees [6].	PASS with local flow alignment and zoning.
D3 - Commercial practicality	AeroSHARK uses ~50 micrometer riblets on hundreds of square meters and reports ~1% aircraft fuel/drag benefit in service [8,9].	PASS at concept/practicality level.

Verdict: ACCEPT as the primary aerodynamic mechanism.

4.5 Idea E - Make riblet scale and orientation zone-specific instead of one-size-fits-all

Attack	Attempt to discredit	Result
E1 - Cruise-condition variation	The optimum physical size changes with nu/u_tau. A fixed physical spacing can move off-design as local Reynolds number changes.	PASS because zoning explicitly maps s+ to local u_tau and viscosity.
E2 - Multi-point operation	Takeoff, climb, cruise and descent have different wall-unit scales. A geometry optimized for one point may lose benefit elsewhere.	PASS conditionally: optimize for mission fuel-weighted cruise states, and require no significant drag penalty at off-design states.
E3 - Manufacturing complexity	Many unique panels increase tooling, inventory and installation errors.	PASS if reduced to a finite family of 4-8 riblet zones with clear flow-direction markings and digital cut files.

Verdict: ACCEPT. This is the main “dramatic improvement” over a generic fixed microtexture because it adapts the geometry to the actual boundary-layer state without active mechanisms.

4.6 Idea F - Add a thin, low-F, multilayer DLC protective nanocoating over riblets

Attack	Attempt to discredit	Result
F1 - F weakens DLC	High fluorine content can reduce hardness and shift the network toward polymer-like carbon [10,11].	PASS by using fluorine only in a thin cap (target ~5-12 at.% F) over a tougher DLC/DLN support.

F2 - Film cracking on flexible riblets	DLC has high modulus and residual stress; flexing a polymer film can crack or delaminate it.	PASS conditionally: keep total hard stack about 0.8-1.5 micrometers, use a compliant Si/O-containing transition layer, low-temperature deposition, and qualify minimum bend radius.
F3 - Riblet rounding	A conformal coating could blunt riblet tips and alter h/s.	PASS if coating thickness is <~2% of riblet spacing and profilometry confirms post-coating geometry within tolerance.

Verdict: ACCEPT as a secondary durability/anti-fouling function, not as the claimed source of aerodynamic drag reduction.

4.7 Idea G - Manufacture the system as a removable film rather than coat the completed aircraft in a vacuum chamber

Attack	Attempt to discredit	Result
G1 - Added mass	A carrier and adhesive add mass, reducing the net fuel benefit.	PASS if areal mass is held near 0.08-0.15 kg/m2; a 600-800 m2 installation then adds roughly 50-120 kg.
G2 - Seams and steps	Panel edges can add roughness and drag.	PASS conditionally with streamwise seams, flush/tapered edge designs, strict step-height limits, and CFD/wind-tunnel seam qualification.
G3 - Adhesive durability	Thermal cycling, fluids, UV, deicing chemicals and moisture can weaken PSA bonds.	PASS only after environmental peel/shear aging and repairability tests; this is a qualification gate.

Verdict: ACCEPT because it solves the source paper’s largest manufacturability problem and mirrors the practical route already demonstrated by commercial riblet films.

5. Final integrated concept: AeroRib-FDLC-X

AeroRib-FDLC-X is a removable, flow-oriented riblet film divided into surface zones. Each zone has a riblet spacing and height selected from a mission-weighted local wall-shear model. The external surface is protected by a sub-2-micrometer graded DLC stack. The design is intentionally hierarchical: millimeter-to-meter aircraft geometry controls pressure drag; 50-100 micrometer riblets modify near-wall turbulence; sub-micrometer DLC chemistry controls wear, adhesion, and surface energy.

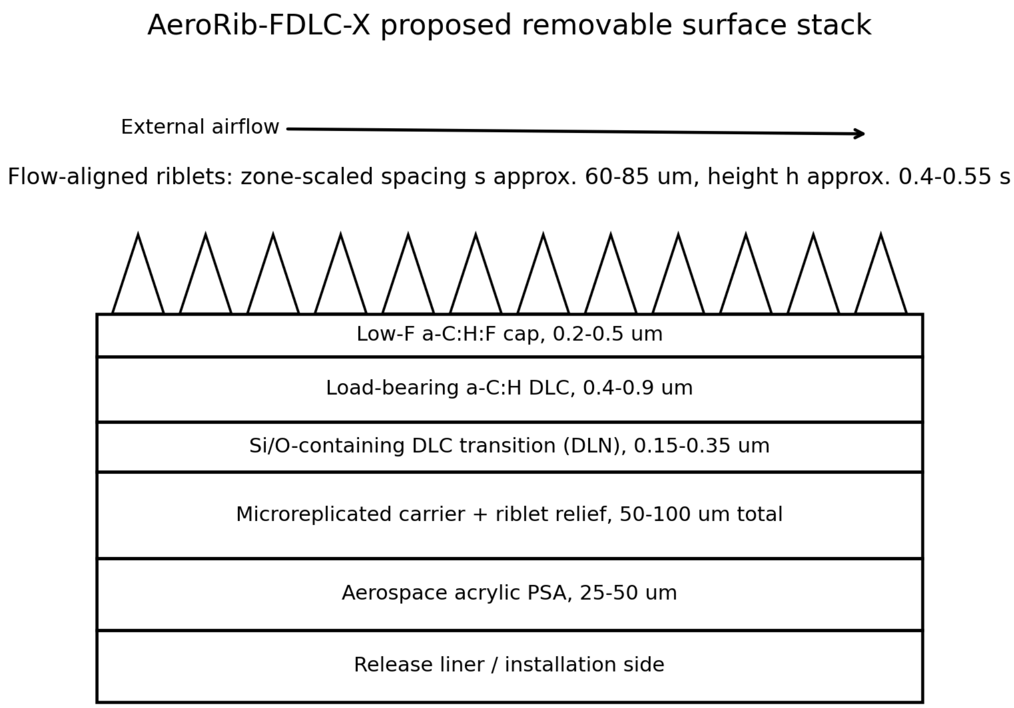

Figure 3. Proposed AeroRib-FDLC-X stack. Dimensions are starting design targets, not certified production values.

5.1 Proposed layer stack and target composition

Layer	Nominal thickness	Representative chemistry / structure	Primary role
Adhesive	25-50 um	Crosslinked aerospace acrylic PSA; e.g., soft acrylate-rich copolymer with small polar comonomer fraction.	Removable structural bond to existing topcoat.
Riblet carrier + relief	50-100 um total	UV-cured aliphatic urethane-acrylate or high-temperature polymer film with microreplicated triangular/trapezoidal ribs.	Creates aerodynamic microgeometry and flexible carrier.
Transition / DLN	0.15-0.35 um	a-C:H:Si:O, graded from organosilicon-rich to carbon-rich.	Stress relief, adhesion, pinhole suppression.
Load-bearing DLC	0.4-0.9 um	a-C:H with mixed sp2/sp3 carbon; target sp3 fraction approximately 40-60%, optimized for stress/hardness rather than maximized.	Wear resistance and geometry retention.
Low-F cap	0.2-0.5 um	a-C:H:F, target F about 5-12 at.% at the top surface; C-F/C-Fx termination.	Lower surface energy, anti-fouling, environmental tribology.

Amorphous DLC does not have a single molecular formula. Its useful chemical specification is therefore an atomic-composition and bonding window rather than a stoichiometric compound formula. For the top cap, a practical shorthand is a-C:H:F(x), where x is controlled to a low fluorine fraction. The design deliberately avoids the source paper's assumption that 10-20 at.% F and ~80% sp3 can simply be specified independently; in F-DLC, fluorine content, sp2/sp3 structure, stress, modulus, and hardness are coupled [10,11].

5.2 Urethane-acrylate riblet matrix chemistry

One manufacturable carrier option is a microreplicated aliphatic urethane-acrylate relief layer cast on a thin film. A generic urethane diacrylate oligomer can be represented by the step-growth reaction:

$$\text{OCN-R-NCO} + 2\ \text{HO-R}'\text{-O-C(O)-C(CH}_3\text{)=CH}_2 \rightarrow \text{CH}_2\text{=C(CH}_3\text{)-C(O)-O-R}'\text{-O-C(O)-NH-R-NH-C(O)-O-R}'\text{-O-C(O)-C(CH}_3\text{)=CH}_2$$

The terminal acrylates are then free-radically crosslinked under UV in a precision negative riblet mold. The chemistry is selected for low shrinkage, hydrolytic stability, UV resistance, and enough toughness that 30-40 micrometer-high riblets survive cleaning and rain erosion. For production, prequalified commercial urethane-acrylate oligomers should be used rather than synthesizing isocyanate prepolymers at the aircraft facility.

5.3 DLC network chemistry and surface-energy mechanism

The DLC layers are metastable amorphous carbon networks containing sp3 tetrahedral and sp2 trigonal carbon. Mechanical hardness generally rises with sp3 fraction, while excessive internal stress can also rise. Fluorine terminates dangling bonds and forms C-F, C-F2 and, at higher fluorination, C-F3 environments. This reduces the polar contribution to surface energy but also tends to reduce network crosslinking and hardness as fluorine content increases [10]. The functionally graded design therefore places most structural duty in a fluorine-poor DLC layer and reserves F for the outer few hundred nanometers.

A 2023 multilayer F-DLC study used Ti/DLN/DLC/f-DLC layers to combine adhesion, mechanical resilience and low surface energy; it reported a Young's modulus around 78 GPa and surface energy around 24 mJ/m2 for its F-DLC architecture and emphasized the value of a Si/O-containing DLN stress-relief layer [10]. The present concept borrows the multilayer logic but modifies thickness, substrate and deposition temperature for a flexible riblet film rather than a condenser tube.

6. Aerodynamic theory and design equations

6.1 Wall-unit scaling

Riblets work only when their physical scale is matched to the viscous near-wall scale. Define friction velocity u_tau and kinematic viscosity nu as:

$$u_\tau = \sqrt{\tau_w/\rho} = U\sqrt{C_f/2}, \qquad \nu = \mu/\rho.$$

The viscous-scaled spacing and height are:

$$s^+ = s\,u_\tau/\nu, \qquad h^+ = h\,u_\tau/\nu.$$

For conventional riblets, published data cluster the useful spacing near O(10-20) wall units, with ~15 often close to optimum depending on geometry [4-7]. Thus the physical spacing is:

$$s = s^+\,\nu / u_\tau = s^+\,\nu / [U\sqrt{C_f/2}].$$

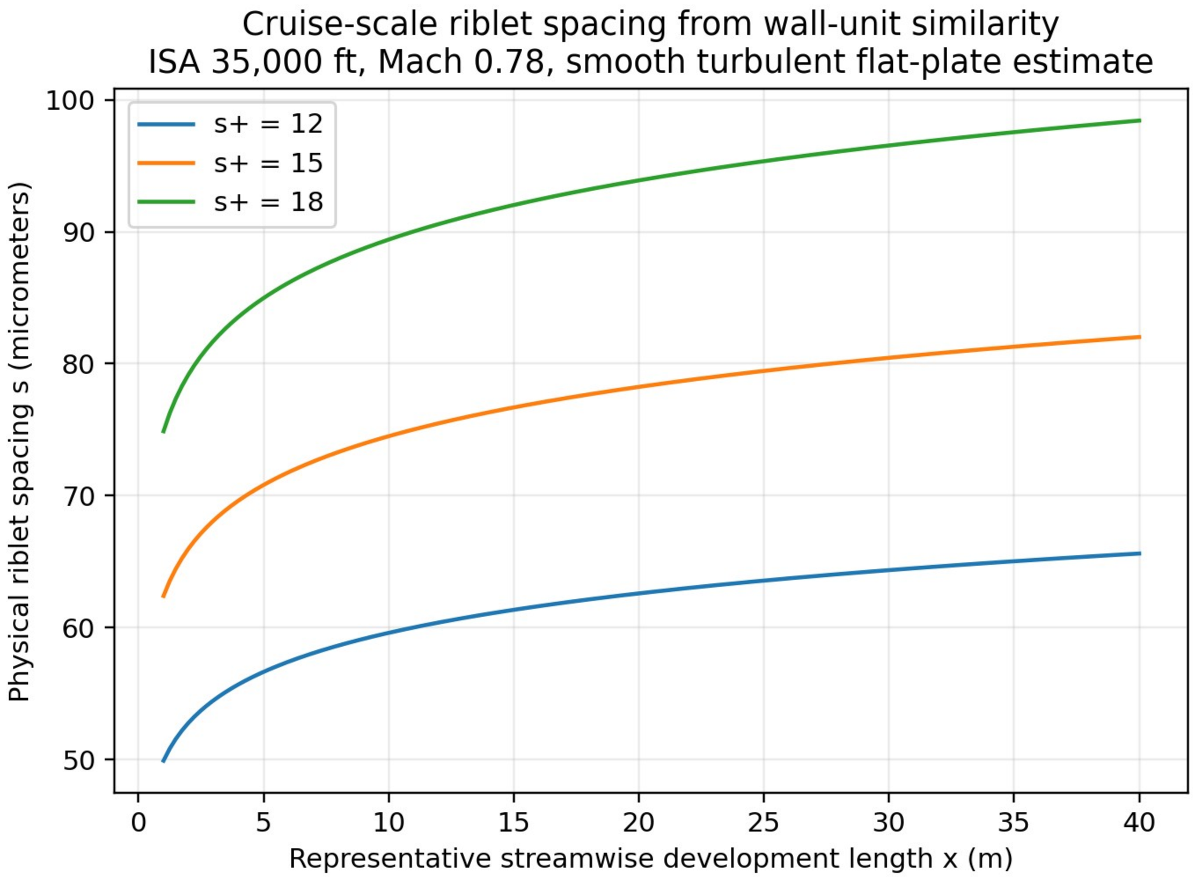

Figure 4. Example physical spacing calculated from s+ similarity at 35,000 ft and Mach 0.78. The slow growth from ~60 to ~85 micrometers illustrates why a finite set of size zones is practical.

6.2 Representative 737-class cruise calculation

For an illustrative single-aisle cruise point at 35,000 ft and Mach 0.78, the standard-atmosphere estimate gives T ≈ 218.8 K, rho ≈ 0.380 kg/m3, mu ≈ 1.43e-5 Pa·s, nu ≈ 3.78e-5 m2/s, and U ≈ 231 m/s. Using the smooth turbulent compressible flat-plate correlation, representative local Cf values fall from about 0.0031 at x = 1 m to about 0.0018 at x = 40 m. For s+ = 15, the corresponding physical spacing increases from roughly 62 to 82 micrometers. A practical four-zone family could therefore use nominal spacings such as 60, 70, 80 and 90 micrometers after local CFD calibration rather than a single universal 50 micrometer rib.

x (m)	Re_x	Cf (estimate)	u_tau (m/s)	s for s+=15 (um)
1	6.13e6	0.00308	9.08	62
5	3.06e7	0.00239	8.00	71
10	6.13e7	0.00216	7.60	75
20	1.23e8	0.00196	7.24	78
40	2.45e8	0.00178	6.91	82

6.3 Riblet cross-section

Initial geometry should use a well-characterized straight triangular or trapezoidal section, not a novel herringbone pattern. A starting design family is h/s = 0.4-0.55 with a sharp but manufacturable tip and a root radius much smaller than the groove spacing. The 2024 yaw study used trapezoidal riblets with h/s =

0.5 and found ~7% maximum drag reduction with little loss below ~10 degrees yaw [6]. Any new cross-section should be benchmarked against this conventional reference before being accepted.

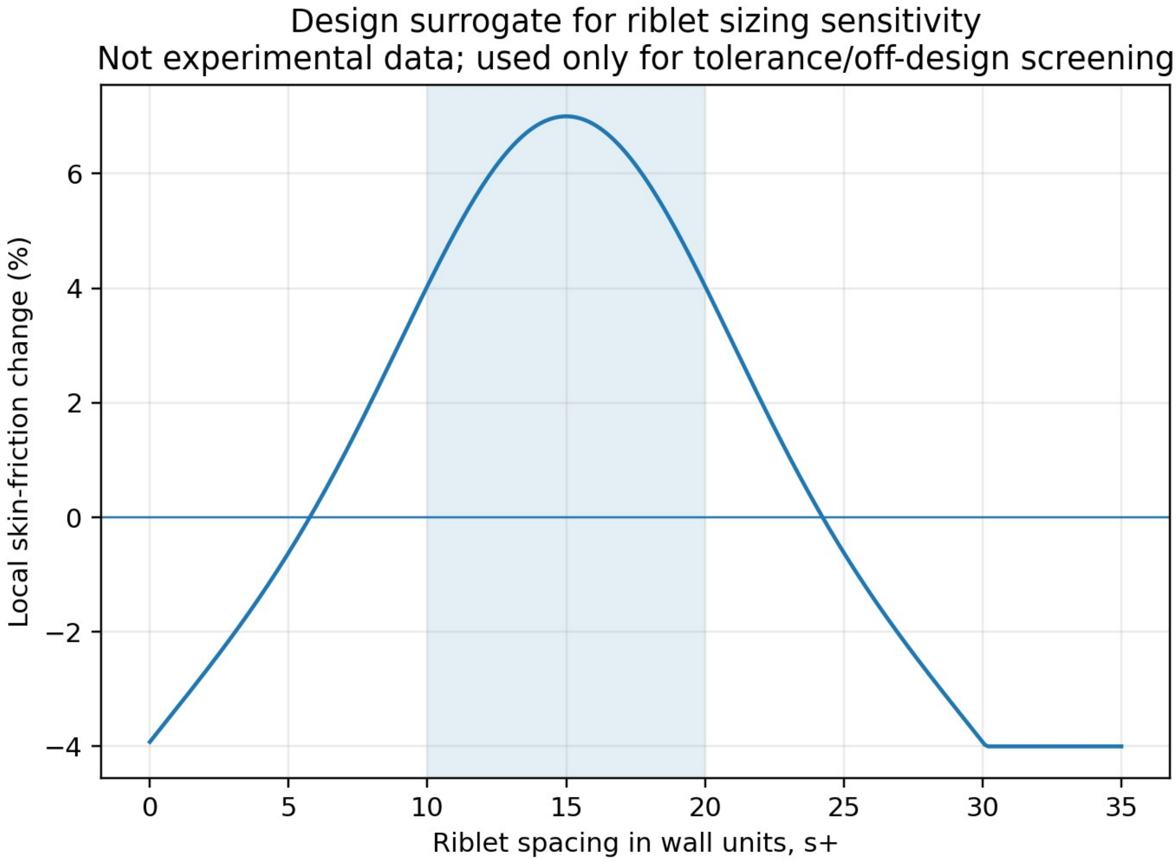

Figure 5. A deliberately labeled design surrogate used for tolerance studies. It is not experimental data and must be replaced by measured geometry-specific curves during development.

6.4 Aircraft-level drag aggregation

A transparent first-order aggregation is preferable to an unexplained CFD curve. Let f_sf be the fraction of total cruise drag due to skin friction, f_cov the fraction of that skin-friction-producing area effectively covered, R_rib the local riblet skin-friction reduction, and eta the realization factor for seams, yaw, roughness, contamination and off-design operation. Then:

$$\text{DeltaD} / D \approx f_{sf} * f_{cov} * R_{rib} * \text{eta}.$$

Using f_sf = 0.45, f_cov = 0.70-0.85, R_rib = 0.06-0.08, and eta = 0.75-0.90 gives a broad concept range of roughly 1.1-2.8% total cruise drag reduction. A narrower development target of 1.3-2.5% is recommended until CFD, tunnel, and flight data are available. This aligns with literature that reports 5-8% local skin-friction reduction, aircraft-level total-drag potential of ~2-3% with broad coverage, and current AeroSHARK operation around 1% at today's coverage stage [4,8,9].

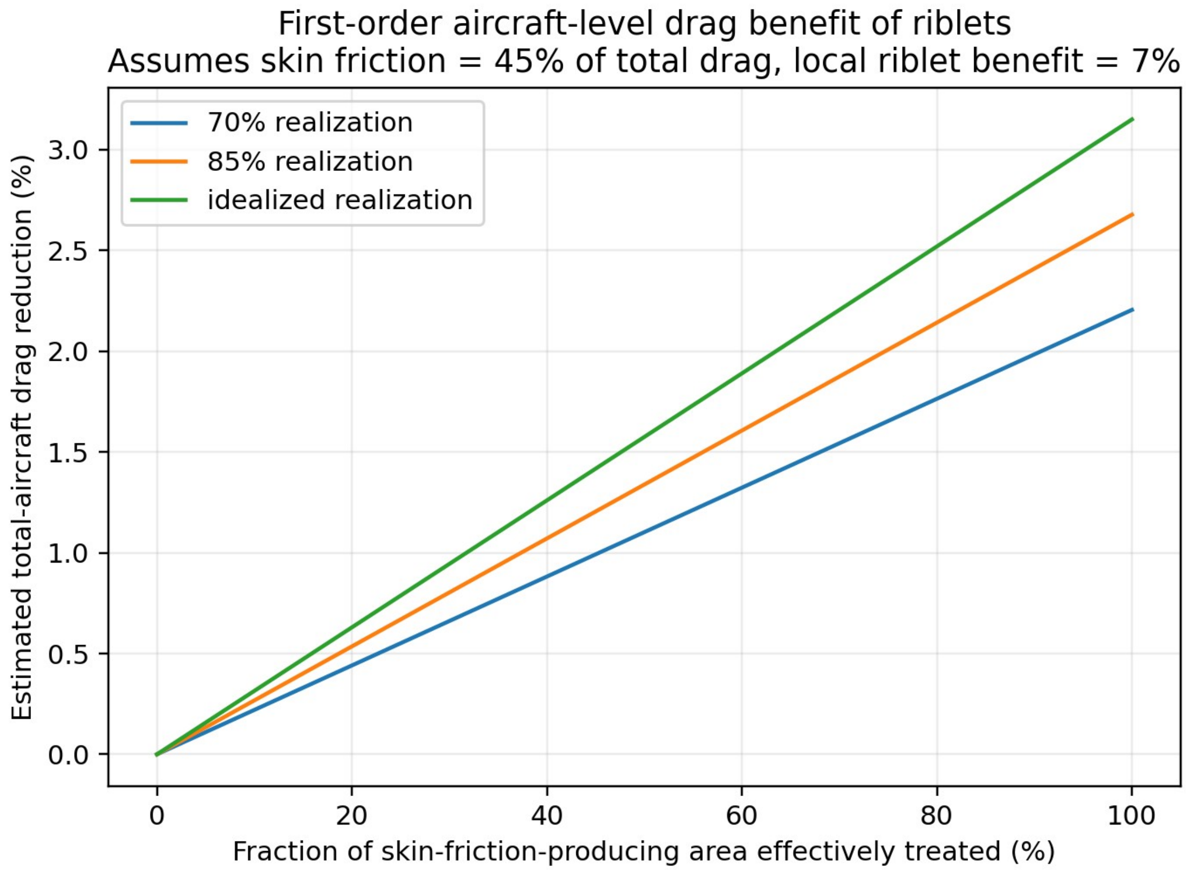

Figure 6. First-order total-aircraft drag reduction as a function of effective coverage. The plot exposes assumptions rather than hiding them inside an undocumented CFD curve.

6.5 Fuel-burn translation

Block-fuel reduction is not exactly equal to cruise drag reduction because takeoff, climb, descent, reserves, payload and engine operating point remain. Define a mission conversion factor k_mission:

$$\text{DeltaF\_block} / \text{F\_block} \approx \text{k\_mission} * \text{DeltaD\_cruise} / \text{D\_cruise}, \quad 0 < \text{k\_mission} < 1.$$

For cruise-heavy missions, a planning range k_mission ≈ 0.6-0.9 is reasonable for early screening; the actual value must come from an aircraft performance model. A 1.5-2.2% cruise drag reduction could therefore correspond to roughly 0.9-2.0% block-fuel reduction depending on route structure. This is why the source paper’s automatic conversion from a claimed 5% drag reduction to 2% fuel savings is insufficient without a mission model.

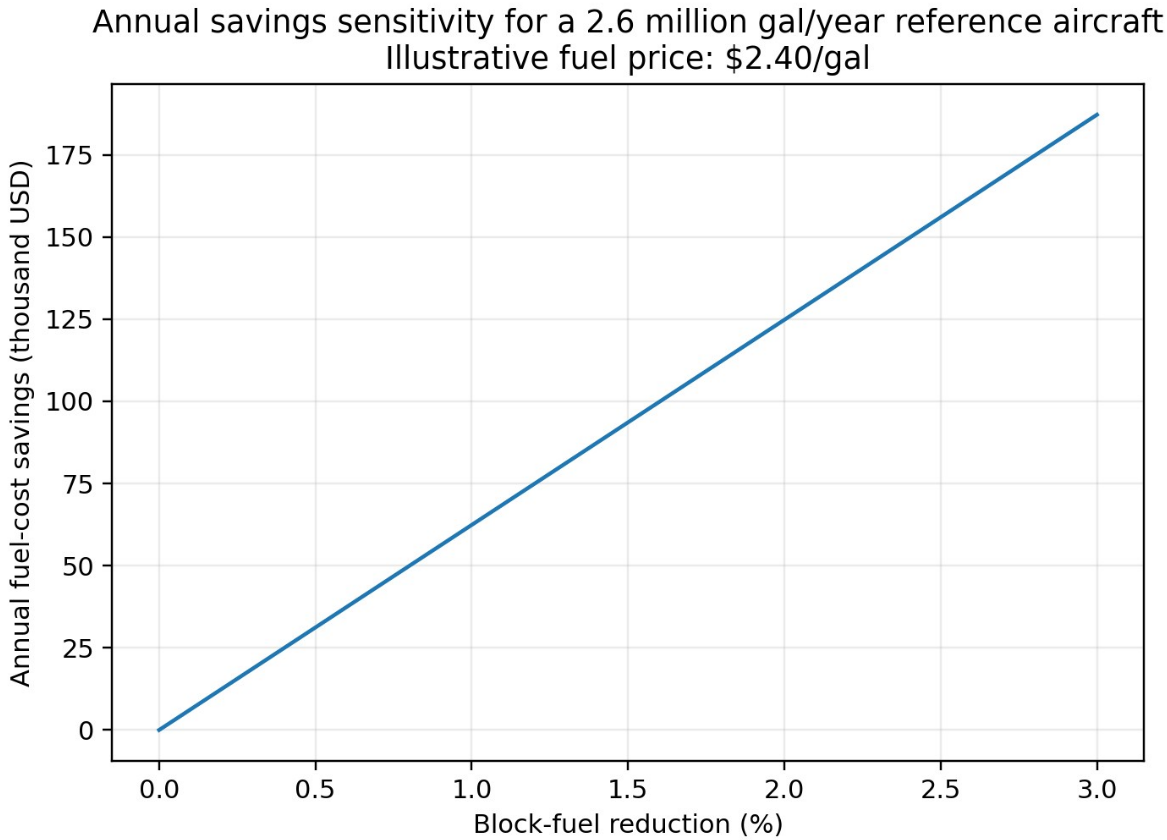

Figure 7. Illustrative savings using the source paper's 2.6 million gal/year reference consumption. Dollar values scale linearly with actual fuel price and utilization.

7. Surface roughness, contamination, and secondary aerodynamic effects

7.1 Roughness budget

The film must be smooth everywhere except for the intentional streamwise riblet relief. Uncontrolled orange peel, particles, seam steps, coating nodules and erosion pits can erase the riblet benefit. The development specification should therefore separate three scales: (1) macro waviness at millimeter-to-meter scale, controlled by installation; (2) riblet-scale periodic geometry, intentionally 50-100 micrometers; and (3) nanoscale coating roughness, targeted at Ra below roughly 50-100 nm where practical. Final acceptable limits must be derived from roughness Reynolds number and wind-tunnel tests rather than from cosmetic paint criteria alone.

7.2 Insect residue and laminar-flow surfaces

NASA has shown that insect residue on leading edges can trigger premature laminar-turbulent transition and increase drag on laminar-flow aircraft [15,16]. The AeroRib-FDLC-X baseline therefore does not place turbulent riblets on a region that must remain laminar. On future natural- or hybrid-laminar-flow wings, the leading-edge solution should instead be an ultra-smooth, low-energy anti-contamination strip, with the riblet film beginning only downstream of the designed transition region. This is an example of why local flow physics must dominate material uniformity.

7.3 Icing

F-DLC can be hydrophobic and has been studied for anti-icing, but hydrophobicity can degrade dynamically as condensation and freezing alter the wetting state [17]. The concept therefore does not claim ice protection as a substitute for certified anti-ice systems. Ice adhesion and icing-delay tests are secondary durability/maintenance metrics only.

8. Manufacturing process - development and scale-up

The recommended architecture is manufactured off-aircraft as coated riblet film. This eliminates the need to place a complete wing or fuselage in a PECVD chamber and makes replacement possible during scheduled maintenance. The following sequence is a development recipe and process architecture, not a production qualification document.

8.1 Step 1 - Aerodynamic surface zoning

1. Create the clean-aircraft outer mold line including paint/fastener/seam geometry for the target configuration.
2. Run RANS/LES-supported CFD at a mission-weighted set of cruise points and at key off-design points. Extract local rho, mu, U_e, tau_w, pressure gradient, surface streamline direction and boundary-layer state.
3. Compute u_tau and candidate s, h from target s+ and h+ values. Cluster the continuous map into 4-8 manufacturable zones while minimizing deviation from the optimum wall-unit range.
4. Exclude regions with unstable crossflow, separation, high leading-edge erosion, antennas/sensors, drains, static ports, or other certification-sensitive features until separately qualified.
5. Generate cut files with orientation arrows and unique zone identifiers.

8.2 Step 2 - Riblet master tooling

6. Fabricate negative masters using diamond machining, precision laser writing, lithographic etching, or electroformed replication tooling.
7. Control pitch to the selected nominal spacing (for example 60-90 um by zone) and h/s to the geometry-specific target (initially 0.4-0.55).
8. Keep tip radius and root radius consistent across the roll; qualify them by white-light interferometry or confocal profilometry.
9. Use a statistical acceptance map over the tool, not a single microscope image. The relevant metric is the distribution of s, h, tip radius, yaw and defect density.

8.3 Step 3 - Microreplication of the carrier

A practical route is roll-to-roll casting of an aliphatic urethane-acrylate formulation against the riblet master, followed by UV cure and release. The formulation should include a weatherable oligomer, low-shrinkage reactive diluent, photoinitiator package, UV stabilizer and, if needed, nanoscale nonagglomerating reinforcement. Filler content must be tightly limited because exposed particles can create aerodynamic roughness. A thin high-temperature polymer backing can be laminated before or after replication to improve handling.

Carrier property	Development target
Areal mass, excluding adhesive	<0.10 kg/m2 preferred
Tensile elongation	Enough to conform to compound curvature without permanent riblet distortion

Glass-transition / heat resistance	Margin above aircraft skin maintenance and service temperatures; compatible with coating deposition
Water uptake	Low and stable
UV/weathering	No cracking, chalking or >5% geometry change after qualification exposure
Riblet geometry retention	<5% change in s and h after cure and lamination

8.4 Step 4 - Plasma surface activation

Before DLC deposition, clean the replicated film in a controlled vacuum/plasma process. A low-energy Ar or Ar/O_2 treatment can remove weak boundary layers and increase adhesion. Polymer heating must be minimized. Published low-temperature DLC processes demonstrate deposition on polymer substrates at room temperature to below about 120 C [13,14]. The exact activation dose must be optimized by peel/scratch performance rather than maximizing plasma power.

8.5 Step 5 - Graded DLN/DLC/F-DLC deposition

A starting low-temperature remote PECVD/PACVD process window is: base pressure below ~0.1 Pa; process pressure of order 1-10 Pa; substrate temperature preferably <120 C; low-to-moderate ion energy; and continuous web cooling. The following sequence is recommended:

10. Deposit ~0.15-0.35 um a-C:H:Si:O (DLN-like) transition layer using an organosilicon precursor such as HMDSO with hydrocarbon/Ar/O_2 tuning. Grade Si/O downward toward the surface.
11. Deposit ~0.4-0.9 um a-C:H load-bearing DLC using a hydrocarbon plasma such as CH_4 or C_2H_2. Tune ion energy for a moderate sp^3 fraction and low residual stress rather than maximum hardness.
12. For only the outer ~0.2-0.5 um, introduce a fluorocarbon precursor and target ~5-12 at.% F at the top surface. The process endpoint is composition and mechanical performance, not a fixed CF_4:C_2H_2 flow ratio because reactor geometry strongly affects incorporation.
13. Cool before winding. Maintain minimum bend radius so the nanolaminate is not strained beyond its qualified limit.

CF_4 can reproduce the historical F-DLC chemistry in R&D, but it should not be the preferred production precursor without point-of-use destruction/abatement and a life-cycle greenhouse-gas analysis because its 100-year GWP is thousands of times CO_2 and its atmospheric lifetime is extremely long [18]. Process development should explicitly search for lower-impact fluorination routes or a fluorine-free cap if equivalent contamination performance can be achieved.

8.6 Step 6 - Adhesive lamination and conversion

14. Laminated PSA should be applied to the back side without embossing or flattening the riblets.
15. Use a release liner with dimensional stability compatible with digital cutting.
16. Die-cut or digitally cut panels so major seams run approximately streamwise where possible.
17. Mark flow direction, zone number, lot number, coating batch, and installation datum on the liner, not the exposed aerodynamic surface.
18. Package panels to prevent riblet crush; no stacking pressure should exceed the qualified compressive load.

8.7 Step 7 - Aircraft installation

19. Inspect existing topcoat for adhesion, corrosion, dents, sealant steps and contamination. Repair out-of-limit defects first.

20. Clean with airframe-approved solvents/cleaners and verify surface cleanliness and dryness.
21. Use laser or template alignment to match the panel orientation to the approved local flow direction. The installation drawing should treat ±5 degrees as a workmanship target even though aerodynamic data may tolerate roughly ±10 degrees.
22. Apply with controlled pressure and no entrapped air. Avoid stretching the panel in the riblet direction.
23. Form tapered/flush seam treatments. Measure seam step height and local riblet yaw after installation.
24. Perform post-installation visual inspection, adhesion witness tests where permitted, and profilometry on representative coupons or accessible witness areas.

9. Quality-control specification

Characteristic	Method	Initial development acceptance target
Riblet spacing/height	Confocal or white-light profilometry	Mean within ±3% of zone nominal; 95% of area within ±5%
Riblet orientation	Optical metrology vs installation datum	Manufactured <±1 deg; installed target <±5 deg locally
Top nanoscale roughness	AFM / optical interferometry on land regions	Ra <50-100 nm target before erosion
DLC thickness	Cross-section SEM or calibrated ellipsometry on witness coupons	0.8-1.5 um total hard stack
Top-layer F content	XPS	5-12 at.% target window
Carbon bonding	Raman + XPS; use TEM/EELS on development coupons if needed	Moderate DLC network; no requirement for an arbitrary 80% sp3 claim
Hardness/modulus	Nanoindentation on rigid witness coupon coated in same run	Hardness target ~15-25 GPa for load-bearing layer, interpreted with substrate effect
Adhesion	Scratch / peel / cross-cut as appropriate to film stack	No delamination under qualified mechanical and thermal loads
Surface energy / wetting	Contact angle + Owens-Wendt or equivalent	Stable low surface energy; low hysteresis preferred
Defect density	Automated optical inspection	No pinholes/particles large enough to violate aerodynamic roughness limit

10. Durability and qualification test program

The concept should be killed early if durability cannot preserve the aerodynamic geometry. The qualification plan must therefore measure riblet shape before and after every environmental test, not merely coating appearance.

Test family	Representative method / condition	Pass criterion
Thermal cycling	Repeated cold-soak/hot-soak cycles spanning expected skin temperatures and maintenance exposures	No blistering/delamination; riblet h and s change <5%; adhesive shear retained.
UV/weathering	Accelerated UV/moisture plus natural exposure	No chalking/cracking; surface energy and geometry remain in spec.

Rain erosion	ASTM G73-style liquid impingement adapted to aircraft speed/angle; include seam coupons	No unacceptable tip rounding, pits, lifting, or seam initiation.
Sand/dust erosion	Particle erosion at representative size distribution and incidence	Local Cf benefit remains positive after damage state.
Cleaning abrasion	Approved brushes/wipes/fluids over repeated maintenance cycles	No progressive riblet flattening or F-DLC delamination.
Hydraulic/fuel/deicing fluids	Immersion/splash per operator materials list	Mass, adhesion and surface geometry stable.
Ice/freeze-thaw	Icing wind tunnel / cyclic frost tests	No delamination; any icephobic benefit treated as secondary.
Lightning/static compatibility	Electrical and system assessment for treated regions	No interference with bonding, static wicks, antennas or lightning paths.
Fire/smoke as applicable	Relevant exterior-material requirements	Meets aircraft certification basis.
Peel/shear aging	Environmental aging followed by peel/shear testing	Safety factor above installation minimum; no creep-induced seam steps.

10.1 Aerodynamic validation ladder

25. Flat-plate channel/wind-tunnel coupon: measure DeltaCf directly for each riblet geometry, yaw angle, surface contamination state, and roughness state.
26. 2D airfoil: evaluate favorable/adverse pressure gradients and confirm no new separation penalty.
27. 3D swept-wing or fuselage panel: quantify crossflow sensitivity and seam effects.
28. High-Reynolds-number pressurized or cryogenic facility where available: preserve flight-like wall-unit scaling.
29. Instrumented flight test on a small panel with direct/indirect skin-friction measurement.
30. Aircraft-level A/B flight program with paired routes, weather normalization, engine health correction, and statistical fuel-burn analysis.

11. Expected properties and performance targets

Property	**AeroDLC-F source claim**	**AeroRib-FDLC-X development target / interpretation**
Direct drag mechanism	Low dry sliding CoF	Riblet-induced reduction in turbulent wall shear
Tribological CoF	~0.03 vs steel	Secondary metric only; no aircraft drag claim derived from it
Local skin-friction reduction	Implied from coating, up to 5% total drag	Target 6-8% local turbulent skin-friction reduction on qualified zones
Aircraft cruise drag reduction	Claimed peak 5%	Concept target 1.3-2.5%, stretch up to ~3% only with broad validated coverage
Block fuel reduction	1-5% claimed	Planning target ~0.8-2.0% depending mission and coverage; must be flight-validated
Surface energy	Not quantified	~20-30 mJ/m2 target for top cap

Hardness	15-25 GPa	~15-25 GPa load-bearing witness-coupon target; top cap can be lower
Thickness	1-5 um directly on aircraft	~0.8-1.5 um hard nanostack on 50-100 um removable riblet film
F content	10-20 at.% throughout	~5-12 at.% only near top surface; graded to near-zero in load-bearing layer
Manufacture	Whole-component PECVD, “robotic spraying” suggested	Roll-to-roll microreplication + low-temperature plasma coating + maintenance installation
Maintainability	Not developed	Panel replacement, seam inspection, local repair, scheduled cleaning criteria

12. Cost, mass, and payback model

12.1 Areal mass

A realistic removable architecture has an aerodynamic benefit only if its mass remains small. Example mass accounting per square meter: 50 um polymer carrier at 1.2 g/cm3 ≈ 0.060 kg/m2; 30 um acrylic adhesive at 1.0 g/cm3 ≈ 0.030 kg/m2; average riblet relief ≈ 0.010-0.025 kg/m2; 1.2 um DLC stack at ~2.2 g/cm3 ≈ 0.0026 kg/m2. Total target is therefore about 0.10-0.12 kg/m2 before liners and installation consumables. A 700 m2 installation would add roughly 70-85 kg. This estimate must be replaced by measured production-film mass.

12.2 Manufacturing and installation cost model

No defensible public price exists for the proposed film, so the paper should use a cost equation rather than invent a precise per-aircraft quote. Define treated area A, finished-film manufacturing cost C_film per m2, installation labor cost C_inst per m2, nonrecurring engineering/certification allocation C_NRE, and maintenance present value C_maint:

$$C\_total = A\ (C\_film + C\_inst) + C\_NRE + C\_maint.$$

For exploratory planning only, if mature production film were $150-300/m2 and installation $75-150/m2 for A = 700 m2, direct recurring installation could be roughly $158,000-$315,000 before operator-specific downtime, engineering, certification and maintenance. This is intentionally broader and likely higher than the source paper’s unsupported $63,000 estimate. A valid program should compare payback against verified fuel benefit, not target an arbitrary low coating price.

12.3 Savings sensitivity

Using the source paper’s own annual consumption example of 2.6 million gal/year and $2.40/gal, each 1% block-fuel reduction is worth about $62,400/year; 1.5% is about $93,600/year; 2.0% about $124,800/year; and 2.5% about $156,000/year. With a recurring installed cost of $200,000, simple payback is ~1.6 years at a 2% fuel reduction, before financing, downtime and maintenance. Conversely, if only 1% fuel reduction is realized, payback exceeds three years. The economics are therefore highly sensitive to real flight data.

13. Certification and operational integration

A certified installation would likely proceed through an STC or type-design change process appropriate to the aircraft and jurisdiction. The technical package must demonstrate that the surface does not adversely affect flight characteristics, structural protection, lightning/static behavior, systems, drainage, icing compliance, markings, maintenance access, or emergency procedures. AeroSHARK's existing in-service implementation is evidence that riblet films can be certified, but it does not transfer certification to this new material stack or to new surface coverage [8,9].

- Create a configuration-controlled surface map identifying approved and prohibited treatment zones.
- Define life limit or on-condition inspection criteria for erosion, seam lifting, contamination and riblet damage.
- Provide structural-repair-manual instructions for removal around fasteners, panels and repairs.
- Prohibit field recoating of the DLC stack; damaged panels should be replaced with serialized approved parts.
- Add cleaning methods that remove contamination without rounding riblet tips.
- Validate paint/film removal chemistry so substrate corrosion protection is not degraded.

14. Remaining failure modes and kill criteria

Failure mode	Why it could kill the concept	Early kill criterion
Riblet erosion	Loss of h/s converts a drag-reducing surface into roughness.	After accelerated erosion, measured DeltaCf must remain positive with margin.
Seam drag	Thousands of edge steps can erase local riblet benefit.	Full seam density included in tunnel model; net panel benefit >3% local Cf reduction.
DLC cracking	Crack ridges can become roughness and moisture pathways.	No crack population large enough to exceed aerodynamic roughness threshold after bend/thermal cycling.
Adhesive creep	Creates blisters/steps and foreign-object risk.	No creep or lift under worst-case thermal/shear aging with safety factor.
Contamination retention	Riblet valleys can trap dirt and negate benefit.	Defined cleaning interval restores >=90% of clean-panel drag benefit.
Off-design yaw/crossflow	Misaligned riblets can lose benefit or add drag.	Mission-weighted CFD map shows >90% of treated area within approved yaw envelope.
Mass/cost	Small fuel benefit may not repay installation.	Verified mission fuel benefit must exceed operator-specific hurdle after added mass and maintenance.
Environmental process burden	PFC emissions can offset climate value.	Life-cycle CO_2e savings remain strongly positive after verified process emissions and abatement.

15. Development roadmap

Phase	Work	Decision gate
0 - Reproduce source baseline	Make smooth F-DLC coupons and independently measure tribological CoF, surface energy, hardness and aerodynamic Cf.	Confirm that low tribological CoF alone does not produce the claimed aerodynamic benefit.

1 - Geometry screening	Fabricate 10-20 riblet geometries in uncoated polymer; wind-tunnel test vs smooth controls.	Select 2-3 robust geometries with >=5% local Cf reduction across target range.
2 - Coating integration	Apply DLN/DLC/low-F caps; repeat metrology and drag tests.	Coating changes riblet drag performance by <10% relative and improves erosion/cleaning life.
3 - Durability	Rain/sand/UV/thermal/fluid/cleaning/ seam aging.	Aged panel retains >=70-80% of initial local drag benefit.
4 - Large panel / curvature	3D wing/fuselage panel with realistic seams and yaw.	Mission-weighted net drag benefit remains positive with installation defects at tolerance.
5 - Flight demonstrator	Instrumented limited-area installation.	Measured skin-friction/pressure behavior agrees with CFD/tunnel uncertainty.
6 - Aircraft A/B trial	Large-area installation and normalized fuel analysis.	Statistically significant block-fuel benefit and acceptable maintenance burden.
7 - Certification / scale	STC/type design, industrialization, fleet economics.	Operator business case and compliance approval.

16. Why this is dramatically better than the source proposal

Dimension	Source AeroDLC-F	AeroRib-FDLC-X
Causal physics	Infers aerodynamic drag from sliding CoF	Uses wall shear, Cf, Reynolds number, wall units and local streamlines
Novelty location	A new “slippery” material	A systems-level coupling of zoned riblets + graded protective nanochemistry + removable architecture
Falsifiability	No quantitative failure criteria	Three attacks per improvement plus explicit kill criteria
Performance claim	5% drag peak without reproducible CFD details	Transparent 1.3-2.5% cruise-drag target derived from published local riblet effects and coverage
Durability	Scratch test mentioned	Rain, sand, cleaning, UV, thermal, fluid, seam and contamination aging tied to retained DeltaCf
Manufacture	Large vacuum coating of aircraft surfaces	Roll-to-roll film manufacture and maintenance installation
Chemistry	Uniform high-F DLC concept	Gradient: tough low-F/zero-F support + thin F cap to balance hardness and surface energy
Environmental accounting	Not discussed	PFC precursor burden explicitly included in lifecycle gate
Certification	“future flight testing”	Staged coupon -> tunnel -> flight -> STC roadmap

17. Conclusions

The original AeroDLC-F idea contains a useful materials insight - fluorinated DLC can combine low surface energy with much greater hardness than PTFE-like polymers - but it attaches that insight to the wrong primary aerodynamic variable. A lower ball-on-disk coefficient of friction does not imply a proportionate reduction in aircraft skin-friction drag. Once that error is corrected, the best route is to let riblet geometry perform the aerodynamic work and let the coating chemistry preserve that geometry and control fouling.

The resulting AeroRib-FDLC-X concept survives the requested three-attack analytical falsification process at the engineering-hypothesis level. Its most defensible performance target is not a magical 5% total-drag reduction from "slipperiness," but a mission- and coverage-dependent 1.3-2.5% cruise drag reduction with roughly 0.8-2.0% block-fuel potential on suitable operations, plus possible maintenance benefits from a harder low-energy surface. The concept becomes scientifically meaningful because every claimed benefit now has a corresponding measurable variable, equation, failure mode, and validation experiment.

The decisive next experiment is straightforward: manufacture otherwise identical smooth, ribleted-uncoated, ribleted-DLC, and ribleted-F-DLC coupons; measure direct skin-friction drag at flight-relevant s+ across yaw and roughness states; then run erosion/cleaning cycles and repeat. If the coated riblet panel does not retain a statistically significant net drag benefit after aging, the concept should be discarded or redesigned before any aircraft-scale investment.

References

[1] "AeroDLC-F: A Novel Perfluorinated Diamond-Like Carbon Coating for Aerodynamic Friction Reduction on Airplane Wings." EquationFarm-hosted PDF, 27 Aug 2025. https://www.equationfarm.com/content/files/2025/08/e4f91aef-cb60-4008-94ba-2c88f368bb6e--1-.pdf

[2] NASA Glenn Research Center. "What is Drag?" Boundary-layer and aerodynamic-friction overview. https://www1.grc.nasa.gov/beginners-guide-to-aeronautics/what-is-drag/

[3] NASA Glenn Research Center. CFPOST User's Guide, skin-friction coefficient definition: Cf = tau/q. https://www.grc.nasa.gov/www/winddocs/cfpost/appc.html

[4] Viswanath, P.R. "Aircraft viscous drag reduction using riblets." Progress in Aerospace Sciences 38 (2002), 571-600. DOI: 10.1016/S0376-0421(02)00048-9.

[5] Walsh, M.J. "Riblets for aircraft skin-friction reduction." NASA Langley, 1986. NTRS 19880005573.

[6] Inasawa, A., Taniguchi, R., Asai, M., et al. "Experimental investigation of yaw-angle effects on drag reduction rate for trapezoidal riblets." Experiments in Fluids 65, 29 (2024). DOI: 10.1007/s00348-024-03763-7.

[7] Amico, E.; Cafiero, G. "A short review of unconventional riblet designs for skin-friction drag reduction in turbulent flows." Chinese Journal of Aeronautics (2026), 104278. DOI: 10.1016/j.cja.2026.104278.

[8] Lufthansa Technik. "LATAM extends AeroSHARK use across entire Boeing 777 fleet." 2026. Reports ~50 um riblets, ~950 m2 on 777-300ER, and proven ~1% drag/fuel benefit in current implementation.

[9] Lufthansa Group. "Operational Efficiency." 2025/2026 update. Reports AeroSHARK current fuel/CO2 reduction of about 1% and future potential up to ~3%.

[10] Hoque, M.J. et al. "Ultra-resilient multi-layer fluorinated diamond like carbon hydrophobic surfaces." Nature Communications 14, 4902 (2023). DOI: 10.1038/s41467-023-40229-6.

[11] Zhang, L., Wang, F., Qiang, L., Gao, K., Zhang, B., Zhang, J. "Recent advances in the mechanical and tribological properties of fluorine-containing DLC films." RSC Advances 5 (2015), 9635-9649. DOI: 10.1039/C4RA14078H.

[12] Wang, J. et al. "Influence of structure evolution on tribological properties of fluorine-containing diamond-like carbon films: From fullerene-like to amorphous structures." Applied Surface Science 457 (2018), 388-395. DOI: 10.1016/j.apsusc.2018.06.249.

[13] Lee, J.-A. et al. "Dramatically enhanced mechanical properties of diamond-like carbon films on polymer substrate for flexible display devices via argon plasma pretreatment." Chemical Physics 529 (2020), 110551. DOI: 10.1016/j.chemphys.2019.110551.

[14] Nakahigashi, T. et al. "Properties of flexible DLC film deposited by amplitude-modulated RF P-CVD." Tribology International 37 (2004), 907-912. DOI: 10.1016/j.triboint.2004.07.007.

[15] Wohl, C.J. et al. "Insect Residue Contamination on Wing Leading Edge Surfaces: A Materials Investigation for Mitigation." NASA, 2011. NTRS 20110015150.

[16] Wohl, C.J. et al. "Flight Testing Surfaces Engineered for Mitigating Insect Adhesion on a Falcon HU-25C." NASA, 2016. NTRS 20160006873.

[17] "Robust and durable superhydrophobic F-DLC coating for anti-icing in aircraft engineering." Surface and Coatings Technology 404 (2020), 126468. DOI: 10.1016/j.surfcoat.2020.126468.

[18] U.S. EPA. "Understanding Global Warming Potentials." Notes CF4 atmospheric lifetime ~50,000 years and 100-year GWP in the several-thousand range. https://www.epa.gov/ghgemissions/understanding-global-warming-potentials

[19] Boeing. 737 Next Generation Airplane Characteristics for Airport Planning, Rev C, Oct 2025, D6-58325-7. https://www.boeing.com/content/dam/boeing/boeingdotcom/commercial/airports/acaps/737NG_REV_C.pdf

[20] West, N., Sammut, K., Tang, Y. "Material selection and manufacturing of riblets for drag reduction: An updated review." Proc. IMechE Part L 232 (2018), 610-622. DOI: 10.1177/1464420716641452.

[21] Benschop, H.O.G.; Breugem, W.P. "Drag reduction by herringbone riblet texture in direct numerical simulations of turbulent channel flow." Journal of Turbulence 18(8) (2017), 717-759. DOI: 10.1080/14685248.2017.1319951.

Appendix A - Explicit derivation of representative riblet size

Using the illustrative cruise state h = 10,668 m, M = 0.78:

31. ISA temperature: T = T0 - L h = 218.8 K.
32. Density from the tropospheric pressure law: rho ≈ 0.380 kg/m3.
33. Dynamic viscosity from Sutherland's law: mu ≈ 1.43e-5 Pa·s; therefore nu = mu/rho ≈ 3.78e-5 m2/s.
34. Speed of sound a = sqrt(gamma R T) ≈ 296.5 m/s; U = M a ≈ 231.3 m/s.
35. At x = 10 m: Re_x = Ux/nu ≈ 6.13e7.
36. Compressible turbulent flat-plate estimate: Cf ≈ 0.00216.
37. Friction velocity: u_tau = U sqrt(Cf/2) ≈ 7.60 m/s.
38. For s+ = 15: s = 15 nu/u_tau ≈ 74.5 um.
39. For h/s = 0.5: h ≈ 37 um.

The same calculation at x = 1-40 m gives ~62-82 um spacing. This is close to the scale of commercial ~50 um riblet films and supports a zoned family rather than a single arbitrary pitch. A real aircraft design must use local CFD wall shear and local viscosity rather than a flat-plate surrogate.

Appendix B - Experimental matrix for the first decisive test campaign

Surface	Condition	Yaw	Wall-unit range	Measurements
Smooth carrier	Clean	0°, 5°, 10°, 15°	s+ sweep 8-25	Direct Cf + profilometry
Smooth carrier	Contaminated	0°, 5°, 10°, 15°	s+ sweep 8-25	Direct Cf + profilometry
Smooth carrier	Post-rain-erosion	0°, 5°, 10°, 15°	s+ sweep 8-25	Direct Cf + profilometry
Smooth DLC	Clean	0°, 5°, 10°, 15°	s+ sweep 8-25	Direct Cf + profilometry
Smooth DLC	Contaminated	0°, 5°, 10°, 15°	s+ sweep 8-25	Direct Cf + profilometry
Smooth DLC	Post-rain-erosion	0°, 5°, 10°, 15°	s+ sweep 8-25	Direct Cf + profilometry
Smooth F-DLC	Clean	0°, 5°, 10°, 15°	s+ sweep 8-25	Direct Cf + profilometry
Smooth F-DLC	Contaminated	0°, 5°, 10°, 15°	s+ sweep 8-25	Direct Cf + profilometry
Smooth F-DLC	Post-rain-erosion	0°, 5°, 10°, 15°	s+ sweep 8-25	Direct Cf + profilometry
Riblet uncoated	Clean	0°, 5°, 10°, 15°	s+ sweep 8-25	Direct Cf + profilometry
Riblet uncoated	Contaminated	0°, 5°, 10°, 15°	s+ sweep 8-25	Direct Cf + profilometry

Riblet uncoated	Post-rain-erosion	0°, 5°, 10°, 15°	s+ sweep 8-25	Direct Cf + profilometry
Riblet DLC	Clean	0°, 5°, 10°, 15°	s+ sweep 8-25	Direct Cf + profilometry
Riblet DLC	Contaminated	0°, 5°, 10°, 15°	s+ sweep 8-25	Direct Cf + profilometry
Riblet DLC	Post-rain-erosion	0°, 5°, 10°, 15°	s+ sweep 8-25	Direct Cf + profilometry
Riblet low-F-DLC	Clean	0°, 5°, 10°, 15°	s+ sweep 8-25	Direct Cf + profilometry
Riblet low-F-DLC	Contaminated	0°, 5°, 10°, 15°	s+ sweep 8-25	Direct Cf + profilometry
Riblet low-F-DLC	Post-rain-erosion	0°, 5°, 10°, 15°	s+ sweep 8-25	Direct Cf + profilometry

The key comparison is not F-DLC versus PTFE in a sliding tribometer. It is net aerodynamic Cf of riblet low-F-DLC versus the same riblet geometry without the coating after identical environmental aging. If the coating cannot preserve or improve the aged aerodynamic result, its added complexity is not justified.

Appendix C - Pre-registration of concept success criteria

- Initial clean riblet panel: >=5% local skin-friction reduction at the design point versus a hydraulically smooth control.
- Mission envelope: no net local drag increase across the approved cruise yaw/Reynolds-number envelope.
- Post-aging: retain >=70-80% of initial drag reduction after the combined environmental cycle.
- Seam-inclusive panel: >=3% local skin-friction reduction after realistic seam density and installation tolerance.
- Large-area aircraft model: predicted cruise total-drag reduction >=1.3% before committing to flight-test hardware.
- Flight test: statistically significant fuel/drag improvement after weather, mass, engine health and route normalization.
- Lifecycle: fuel/CO2e benefit remains strongly positive after film manufacture, PFC process emissions, added mass, replacement frequency and disposal.